Journal of Controlled Release 155 (2011) 331–340

Contents lists available at ScienceDirect

Journal of Controlled Release

journal homepage: www.elsevier.com/locate/jconrel

Role of boronic acid moieties in poly(amido amine)s for gene delivery

Martin Piest, Johan F.J. Engbersen *

Department of Biomedical Chemistry, MIRA Institute for Biomedical Technology and Technical Medicine, Faculty of Science and Technology, University of Twente, P.O. Box 217, 7500 AE Enschede, The Netherlands

ARTICLE INFO

Article history:
Received 27 May 2011
Accepted 6 July 2011
Available online 18 July 2011

Keywords:
Poly(amido amine)
Phenylboronic acid
Gene delivery
Polyplex
Bioreducible polymer

ABSTRACT

The effects of the presence of two different types of phenylboronic acids as side groups in disulfide-containing poly(amido amine)s (SS-PAA) were investigated in the application of these polymers as gene delivery vectors. To this purpose, a *para*-carboxyphenylboronic acid was grafted on a SS-PAA with pending aminobutyl side chains, resulting in p(DAB–4CPBA) and an *ortho*-aminomethylphenylboronic acid was incorporated through copolymerization, resulting in p(DAB–2AMPBA). Both polymers have 30% of phenylboronic acid side chains and 70% of residual aminobutyl side chains and were compared with the non-boronated benzoylated analogue p(DAB–Bz) of similar M_w. It was found that the presence of phenylboronic acid moieties improved polyplex formation with plasmid DNA since smaller and more monodisperse polyplexes were formed as compared to their non-boronated counterparts. The transfection efficiency of polyplexes of p(DAB–4CPBA) was approximately similar to that of p(DAB–Bz) and commercial PEI (Exgen), both in the absence and the presence of serum, indicating that p(DAB–4CPBA) and p(DAB–Bz) are potent gene delivery vectors. However, the polymers with phenylboronic acid functionalities showed increased cytotoxicity, which is stronger for the *ortho*-aminophenylboronic acid containing polyplexes of p(DAB–2AMPBA) than for the p(DAB–4CPBA) analog. The cytotoxic effect may be caused by increased membrane disruptive interaction as was indicated by the increased hemolytic activity observed for these polymers.

1. Introduction

Gene therapy is a promising technique to cure various metabolic diseases by administration of a therapeutic "healthy" gene to compensate for a malfunctioning gene in the cell. The greatest challenge in gene therapy is the delivery of the therapeutic genes into the targeting cells, and many studies have been performed during last decades to improve this process using viral, liposomal, and polymeric vectors [1]. For example, adeno-associated or recombinant viral vectors are characterized by highly efficient transfection and long-term gene expression, but viral vectors are also plagued by potential risk on safety and immune responses [2]. On the other hand, cationic polymeric vectors are considered to be safer, but generally show much lower efficiency [3–7]. In this category, one very interesting class of materials are poly(amido amine)s (PAAs), since their synthesis by poly-Michael addition of primary or bis(secondary) amines to bis(acrylamides) allows for large structural variation of the main chain and side chains of the polymer. These polymers are typically well soluble in water and their structure can be tuned to form stable nanoparticles that can be used for delivery of a great variety of therapeutic molecules including peptides, plasmid DNA, and siRNA [8].

Previously, our group has developed a broad range of disulfide-based poly(amido amine)s (SS-PAAs) for the delivery of therapeutic plasmid DNA. We showed that the presence of repetitive disulfide bonds in the polymer main chain facilitated the DNA release in the reductive environment of the cytosol through disulfide bond reduction, causing fast degradation of the polymer [9–13]. The charge density of the polymer can be relatively tuned by introduction of aminobutyl side chains that can be partially acylated, as was shown in a recent study for poly(cystamine bisacrylamide/diaminobutane) (abbreviated as p(DAB)) [14]. In the present study we have investigated the effects of the presence of phenylboronic acids in the side chains of SS-PAAs on DNA condensation and transfection properties. Boronic acids are a class of compounds that have interesting binding properties to vicinal diols, notably carbohydrate moieties, and an overview of boronic acid chemistry is presented in Scheme 1.

Boronic acids are the organic derivatives of boric acid and one of the most important properties is their possibility of reversible ester bond formation with alcohols, preferably cis-1,2- and 1,3-diols. The resulting boronic ester can be neutral sp^2 hybridized or anionic sp^3 hybridized and the equilibrium is depending on the pK_a of the alcohol moieties, the pK_a of the boronic acid (typical 10 for alkylboronic acids) and the local environment. It was found that (substituted) phenylboronic acids can form boronic esters at lower pH, since the

* Corresponding author. Tel.: +31 53 489 2926; fax: +31 53 489 2479.
E-mail address: j.f.j.engbersen@utwente.nl (J.F.J. Engbersen).

0168-3659/$ – see front matter © 2011 Elsevier B.V. All rights reserved.
doi:10.1016/j.jconrel.2011.07.011

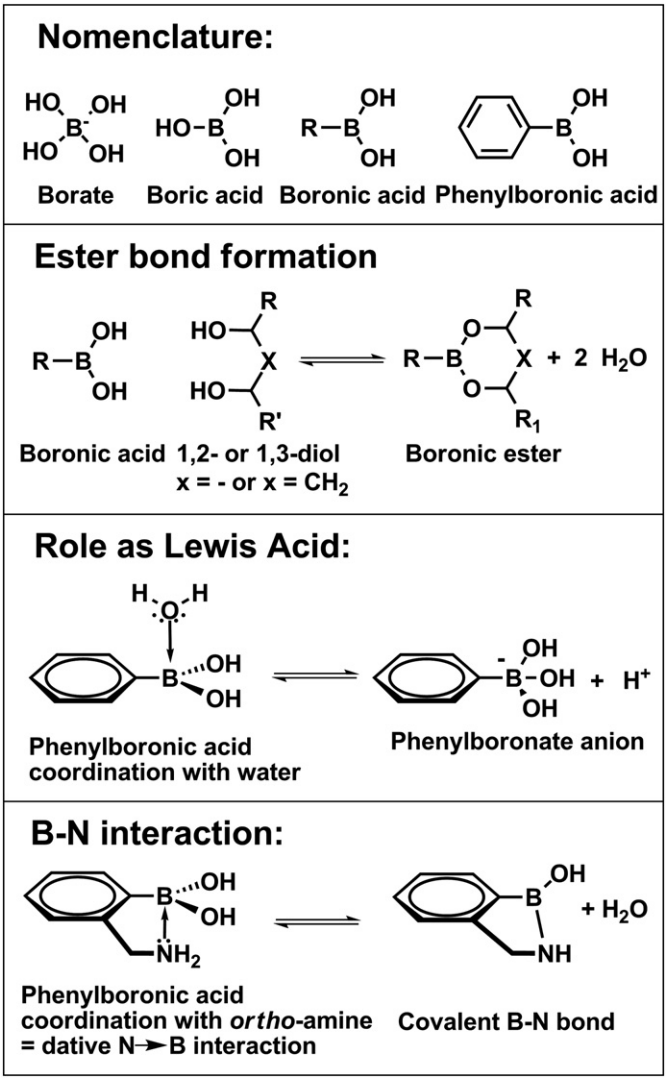

Scheme 1. Overview of boronic acid chemistry.

phenyl ring increases the electron deficiency of the boron centre and increases its role as Lewis acid [15]. In addition, an amine group in the *ortho* position with respect to the boronic acid can significantly increase the pK_a of the boronic acid (from *ca.* 9 to >11) and decrease the pK_a of the secondary amine (from *ca.* 9 to 5) through formation of a dative boron nitrogen bond [16]. This so-called dative B–N (or N→B) interaction could enhance diol complexation at physiological pH.

Over the years, phenylboronic acids have been widely applied in sensor technology for recognition of sugars [17–22], and for the purification of RNA nucleotides and nucleic acids [23–27]. In the biomedical field phenylboronic acid containing polymers have been used for recognition of L-DOPA [28] and for glucose-responsive delivery of insulin [29–33]. Polymers with boronic acid functionalities have also been used for affinity chromatography [34] and some boronic acid containing compounds can act as enzyme inhibitors [35,36]. In addition, boronic acid compounds are known to interact with cells [37–39] and more specifically with the glycoproteins on the cell surfaces [40]. From the perspective of possible targeting applications, it is of particular interest that the phenylboronate function has a relatively high complexation ability for sialic acid (*ca.* 7 times higher than that for glucose) [41]. Sialic acid is a negatively charged sugar that is over-expressed as the terminal group of glycans on the surface of various types of malignant and metastatic cancer cells [42]. This enables to target specifically to tumor cells through the formation of reversible covalent binding between the diol-function of the sialic acid moieties and the boronate functions of the polymers [43].

However, boronic acids have been scarcely studied in the field of gene delivery; the only examples are found in the work of Moffat et al., who utilized the reversible boronic ester bond formation between a salicylhydroxamic acid functionalized PEI and a phenyl(di)boronic acid functionalized PEG for *post*-PEGylation of PEI/DNA polyplexes [44,45], and very recently Peng et al. showed that modification of 1800 Da polyethyleneimine (PEI) with phenylboronic acid groups improved gene transfection [46]. No studies have been performed on the effects of boronic acids in poly(amido amine) gene delivery vectors in relation to cellular uptake and transfection efficiency of boronated polyplexes. Therefore, we aimed to explore the effects of boronic acids in SS-PAAs for gene delivery, since several interactions may play a role in polyplex formation and cell interaction of which a conceptual overview is given in Scheme 2.

In this study the effects of the presence of two different phenylboronic acid moieties in the SS-PAAs polymers p(DAB–4CPBA) and p(CBA–2AMPBA) on their properties as gene delivery vectors have been evaluated. In these polymers, ca. 30% of the aminobutyl side groups of the parent polymer pDAB are functionalized with *para*-carboxyphenyl boronic acid and *ortho*-aminomethylphenylboronic acid, respectively. For comparison, also the nonboronated analogue p(DAB–Bz), with a benzoyl group grafted on 30% of the aminobutyl side chains was prepared. The 30% degree of functionalization was selected since higher degrees were found to reduce too much the polymer solubility [14]. The structures of these polymers and the synthesis routes are given in Schemes 3 and 4. Both boronated SS-PAAs could be relevantly compared with the non-boronated analogue p(DAB–Bz), as their M_w and degree of functionalization were similar. From literature data it is known that an amine in the *ortho* position relative to the boronic acid as is present in p(CBA–2AMPBA) can give a B–N interaction that enhances the binding affinity of the boronic acid for vicinal diol groups as are present in carbohydrates [16,32]. Therefore, it was interesting to evaluate whether possible effects of boronic acid moieties in the SS-PAAs would appear more dominant for p(DAB–2AMPBA) than for p(DAB–4CPBA).

2. Materials and methods

N,N′-cystamine bisacrylamide (CBA, Aldrich), N-BOC-1,4-diaminobutane (Aldrich), benzoylchloride (Aldrich), 2-formylphenylboronic acid (Aldrich) and 4-carboxyphenylboronic acid (Aldrich) were of commercial grade and used without further purification. All reagents and solvents were of reagent grade and were used without further purification.

NMR spectra were recorded on a Varian Unity 300 (^{1}H NMR 300 MHz) using the solvent residual peak as the internal standard. ES-TOF-MS spectra were recorded on a Waters/Micromas LCT mass spectrometer and MALDI-TOF spectra were recorded on a Applied biosystems Voyager DE-RP mass spectrometer.

2.1. Synthesis of the phenylboronic acid functionalized poly(amido amine)s p(DAB–4CPBA) and p(DAB–2AMPBA) and the reference polymer p(DAB–Bz)

The synthesis routes for p(DAB–4CPBA) and p(DAB–Bz) are given in Scheme 3, and for p(DAB–2AMPBA) in Scheme 4. Details of the synthetic procedures are given in the supplementary materials section. Polymers were purified using an ultrafiltration membrane (M_WCO 3000 g/mol). Structure and composition of the polymers were confirmed by ^{1}HNMR and mass spectra (see supplementary materials section).

2.2. Determination of the buffer capacity of the polymers

The buffer capacity of the SS-PAAs was determined by recording the pH change during the automated titration of a concentrated acidic polymer solution with 0.1 M NaOH solution. Therefore, 0.05 g of

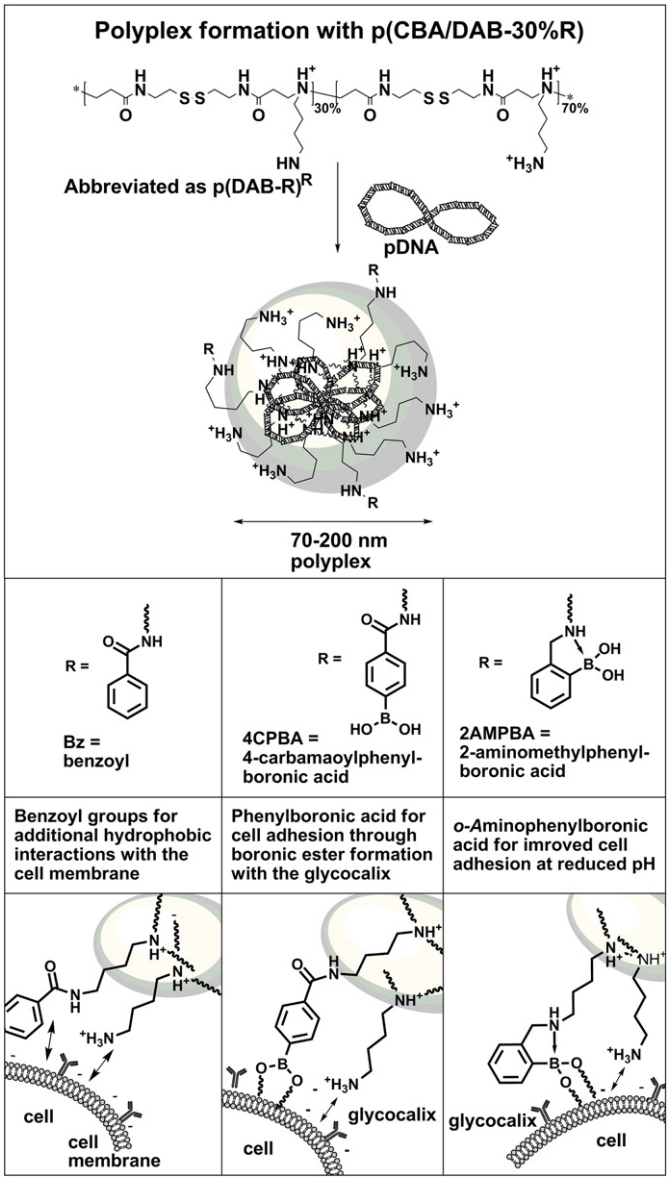

Scheme 2. Boronic acid containing SS-PAAs for gene delivery. Top: polyplex formation with DNA. Bottom: different interactions of the benzoyl or phenylboronic acid groups in the polymer side chains.

polymer (0.25 mmol of protonable nitrogens) was dissolved in 5 ml of 150 mM NaCl solution and the pH was set to 2.0 with a few drops of 1.0 M HCl. This solution was titrated with 0.1 M NaOH solution (0.4 ml/min) and the pH was recorded as a function of the added sodium hydroxide solution.

The buffer capacity is defined as the percentage of (protonable) nitrogen atoms in PAA that becomes protonated in the pH interval from 7.4 to 5.1, being the pH change the polyplexes experience upon change from the extracellular environment (pH 7.4) to the late endosomal environment (pH 5.1). The buffer capacity can be calculated as the mol OH^- added per mol of protonable N-atoms of the polymer, according to Eq. (1).

$$\text{BufferCapacity}(\%) = \frac{(\Delta V_{pol} - \Delta V_{NaCl}) \times 0.1\text{M}}{\text{molN}} * 100\% \quad (1)$$

Where ΔV_{pol} and ΔV_{NaCl} are the volumes of 0.1 M NaOH added to change the pH from 5.1 to 7.4 in the polymer solution and pure 150 mM NaCl solution, respectively. ΔV_{NaCl} was measured and found to be negligible in this pH range. Mol N is the total amount of protonable nitrogen atoms.

2.3. Polyplex preparation

The DNA plasmid solution (1 mg/ml) as supplied by manufacturer was diluted to a final concentration of 0.075 mg/ml in HEPES buffer solution (50 mM, set to pH 7.4). A series of polymer solutions of different concentrations was prepared by dilution of a solution of 0.9 mg/ml in HEPES buffer solution repeatedly 1:1 with HEPES buffer solution. To prepare polyplexes at 48/1, 24/1, and 12/1 polymer/DNA weight ratio 0.80 ml of each polymer solution was added to 0.20 ml of DNA solution in a 1.5 ml Eppendorf tube. The solutions with the polyplexes were vortexed for 5 s and incubated for 30 min at ambient temperature prior to use.

2.4. Determination of polyplex properties by dynamic light scattering (DLS)

Size and zeta potential of the nanoparticles formed by spontaneous self assembly of the poly(amido amine) nanoparticles and of the poly(amido amine)/plasmid DNA polyplexes were measured at 25 °C on a Zetasizer Nano (Malvern Instruments Ltd, Malvern, UK) and the dynamic light scattering results were processed using Dispersion Technology Software V5.0.

2.5. AFM analysis of particle formation

Samples were prepared on freshly cleaved mica using a mixed solution of DNA (0.015 mg/ml final concentration) and polymer (0.72 mg/ml final concentration) resulting in polyplexes of 48/1 polymer/DNA weight ratio in HEPES (20 mM, pH 7.4). The solution was mixed on the mica surface and a total volume of 0.5 μl was used. Polyplex formation was studied using a Veeco Nanoscope III controller in tapping mode. Tapping mode imaging was performed *in situ* in HBS, using a standard liquid cell and a standard Veeco NP cantilever.

The solutions for polyplex formation were mixed directly on the sample surface and after temperature stabilization imaging was started. The formation was monitored for 3 h and partial DNA condensation took place, next the substrate was left to dry overnight while the DNA condensation process was finalized. After drying overnight the polyplexes on mica were studied using tapping mode in air (Nanosensors PPP-NCH-W cantilever). Images were recorded with a scan rate of 1 Hz.

2.6. Determination of DNA condensation using ethidium bromide fluorescence

The efficiency of DNA condensation was measured using the ethidium bromide fluorescence assay as previously described, using a Varian Eclipse fluorescence spectrophotometer, with excitation and emission wavelength of 520 and 600 nm, respectively [13]. Briefly, the fluorescence intensity of a solution of ethidium bromide (5×10^{-6} M) in the presence of uncondensed DNA (0.015 mg/ml) in HEPES (20 mM, pH 7.4) was determined by fluorescence spectroscopy. The molar ratio of ethidium bromide to the DNA phosphates in this solution is 1:10, resulting in intercalation and strong fluorescence of the ethidium cation. Similarly, ethidium fluorescence is measured in the presence of the appropriate solutions containing the polyplexes, using the same concentrations of ethidium bromide and DNA. The relative fluorescence (F_r) represents a relative measure for the degree of shielding of DNA in the polyplex, and was determined from the equation: $F_r = (F_{obs} - F_e)/(F_0 - F_e)$. Here F_{obs} is the fluorescence of the polyplex dispersion, F_e is the fluorescence of ethidium bromide in the

absence of DNA, and F_0 is the initial fluorescence of DNA/ethidium bromide in the absence of polymer.

2.7. In vitro transfection and cell viability

Transfection and cell viability studies were carried out with COS-7 cells (SV-40 transformed African Green monkey kidney cells). Plasmid pCMV-GFP DNA was used as the reporter gene. Two parallel transfection series, one in the presence of serum and one in the absence of serum, were carried out in separate 96–well plates, $n = 6$. The determination of reporter gene expression (GFP) and the evaluation of the cell viability by XTT assay were carried out with the same samples. Polyplexes with polymer/DNA weight ratios 6/1, 12/1, 24/1 and 48/1 were used in the transfection experiments and compared with polyplexes of linear PEI (Exgen 500) at its optimal 6/1 N/P ratio as reference.

In a typical transfection experiment, cells were plated with 10,000 cells per well 24 h prior to use and were >80% confluent. The next day, the cells were incubated with the desired amount of polyplexes (100 μl dispersion with 1 μg plasmid DNA per well) for 2 h at 37 °C in a humidified 5% CO_2-containing atmosphere. Next, the polyplex dispersion was removed, and the cells were washed with 100 μl PBS before 100 μl of fresh culture medium was added and the cells were cultured for another 48 h. The fluorescent intensity of the cells was measured on a TECAN Safire^2 plate reader using SW Magellan Software V6.4. Excitation was at 480 nm and optimal emission was determined at 503 nm.

The cell viability was measured using an XTT assay, in which the XTT value for untreated cells (cells not exposed to the transfection agents) was taken as 100% cell viability. XTT measurements were performed in triplicate using the Perkin Elmer LS50B luminescence spectrometer and analyzed in Kineticalc for Windows V2.0. The absorbance was measured at 490 nm with a reference at 655 nm.

2.8. Erythrocyte leakage

The hemolytic activity of polymers was measured according to literature procedure [14]. A polymer dilution series in HBS (20 mM HEPES, 130 mM NaCl, pH 7.4) was prepared, starting from 1.25 mg/ml to 2.44 μg/ml (10 dilutions). Buffer solution containing 1% Triton X-100 was used as positive control; buffer only was used as a negative control. Polymer and control solutions were filled out in a V-bottom 96-well plate, 100 μl per well. Human erythrocytes were isolated from fresh citrate treated blood, washed in phosphate-buffered saline (PBS) by four centrifugation cycles, each at 800 g for 10 min at 4 °C. The erythrocyte pellet was diluted 10-fold in 150 mM NaCl and 25 μl erythrocyte suspension was added to each well. The plates were incubated at 37 °C for 30 min under constant shaking and the plates were centrifuged at 300 g for 10 min. Next, 60 μl of the supernatant was transferred to a new flat bottom 96–well plate and analyze for hemoglobin content at 405 nm on a TECAN Safire^2 plate reader using SW Magellan Software V6.4.

3. Results and discussion

3.1. Polymer synthesis

In our previous studies of disulfide containing poly(amido amine)s (SS-PAAs) as gene delivery vectors, it was shown that the presence of bioreducible disulfide linkages in these polymers results in significant increases in transfection efficiency together with a reduction in cytoxicity [9–13]. In this study two SS-PAAs with different phenylboronic acid functionalized side chains were compared with the benzoylated reference polymer p(DAB–Bz).

The polymers p(DAB–Bz) and p(DAB–4CPBA) were prepared according to the synthesis route given in Scheme 3 from the same batch of p(DAB). This parent polymer p(DAB) with M_w of 3.5 kDa was prepared by Michael addition polymerization of N,N′-cystamine bisacrylamide and N-BOC protected 1,4-diaminobutane followed by deprotection of the pending amines. For p(DAB–5CPBA), 30% of the aminobutyl groups of p(DAB) were functionalized using an EDC/NHS coupling with 4-carboxyphenylboronic acid. For p(DAB–Bz), 30% of the aminobutyl groups of p(DAB) were benzoylated with benzoyl chloride, resulting in the non-boronated reference polymer p(DAB–Bz).

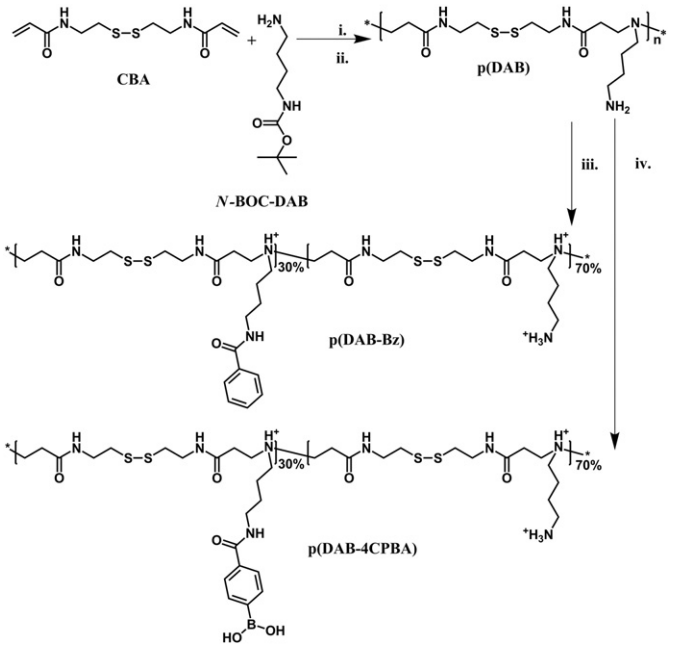

Scheme 3. Michael addition polymerization of CBA with N-BOC-1,4-DAB (i), followed by deprotection with HCl (ii) yields the aminobutyl-functionalized p(DAB). Subsequent functionalization of 30% of the amino groups with benzoyl chloride (iii) or functionalization with 4-CPBA through EDC/NHS coupling (iv), yield p(DAB–Bz) and p(DAB–4CPBA), respectively.

The introduction of the *ortho*-(aminomethyl)phenylboronic acid moieties according to Scheme 4 was achieved by the copolymerization of N,N′-cystamine bisacrylamide with the boronated monomer 1 (20%) and N-BOC 1,4-diaminobutane (80%). The polymer was end-capped with excess of monomer 1, followed by a deprotection step with HCl (g), resulting in polymer p(DAB–2AMPBA). All polymers were obtained in good yields (52–86%) and their structure and composition were confirmed by ^{1}HNMR (Figure S1) and mass spectra (see supplementary materials section).

3.2. Influence of boronic acid groups on the polymer properties

For all three polymers both the M_w and the degree of functionalization are approximately similar, therefore differences in the polymer behavior such as solubility, pH profile, and the tendency for self-aggregation can be attributed primarily to differences in the side group functionality. The pH profiles of the polymers were determined by pH titration experiments and it was observed that all three polymers had a similar pH profile, as is shown in Fig. 1.

It has been observed in our previous studies on SS-PAAs that the buffer capacity of the polymers positively correlates with the transfection efficiency [11]. It is assumed that polymers with a high content of tertiary and secondary amines can buffer the endosomal acidification (proton sponge theory). This results in additional polymer protonation invoking increased charge interactions that can

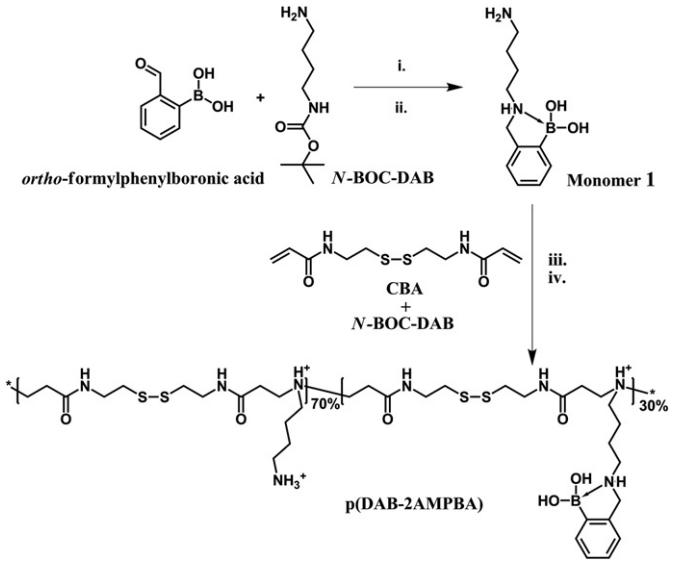

Scheme 4. Reductive amination of 2-formylphenylboronic acid to N-BOC-1,4-DAB (i) and deprotection with HCl (ii) yields monomer 1. Michael addition polymerization of CBA with N-BOC-1,4-DAB and monomer 1 (iii), followed by deprotection with HCl (iv), yields p(DAB–2AMPBA).

destabilize the endosomal membrane, thereby facilitating endosomal escape [44–46]. The buffer capacity is defined as the percentage of titratable amines that becomes protonated the pH range 7.4 (physiological pH) to 5.1 (pH of the late endosome/lysosome).

From the upper part of the curves in Fig. 1 it is apparent that the pK_a values of the primary amine groups in the side chains of the p(DAB) derivatives are typically around 10, as expected for primary amines. Therefore these groups do not contribute to the buffering of the polymers in the endosomal pH range. In contrast, the tertiary amines in the backbone of these polymers have pK_a values in the range of 6.5–7.0 and consequently the relative percentage of protonation/deprotonation of these amines is determining the buffer capacity of the polymer in the endosomal pH range. Since the degree of grafting is similar, differences in buffer capacity between p(DAB–Bz) and p(DAB–4CPBA) can be contributed solely to the presence of the boronic acid functionality in the latter polymer.

As is shown in Table 1, the buffer capacities of the boronated polymers p(DAB–4CPBA) and p(DAB–2AMPBA) are significantly lower than that of p(DAB–Bz) (44% and 36% compared to 62% respectively). The relatively high buffer capacity of p(DAB–Bz) can be attributed to the spontaneous formation of nanoparticles in solution that induce differences in the microenvironment of the tertiary amino groups in the main chain of the polymer. The spontaneous formation of nanoparticles by these polymers in neutral aqueous solution was confirmed by dynamic light scattering (DLS) experiments (*vide infra*, Table 1). It may be assumed that at neutral pH most of the tertiary amino groups are buried in an unprotonated form in the hydrophobic microenvironment of the nanoparticles. At decreasing pH the protonation of the polymer backbone induces an increasing hydrophilicity in the nanoparticles and the increase in hydration of the polymer further shifts the tertiary amines towards increasing protonation.

The lower buffer capacity of the boronated polymers p(DAB–4CPBA) and p(DAB–2AMPBA) indicates that the presence of boronic acids affects the protonation equilibrium of the tertiary amino groups in the main chain. As is shown in Scheme 1, boronic acids are in equilibrium with their boronate anions after coordination with a molecule of water and the release of a proton. The pK_a of phenylboronic acid for this equilibration is reported to be 8.8 [15], whereas the presence of a dative B–N interaction is reported to decrease the pK_a of the ortho amino group to *ca.* 5 [16]. In the titration curves of solutions of both p(DAB–4CPBA) and p(DAB–2AMPBA) no additional buffering is observed in the range pH 7–9, indicating that apparently no free boronic acid is present. A possible explanation for this phenomenon is that the boronic acid groups form a dative B–N interaction with neighboring unprotonated amines (primary, secondary or tertiary) resulting in decrease of pK_a of the amines and an increase of pK_a of the boronic acids to values above 11 [16]. The enhanced pK_a is further based on the possibility of the boronate anion to form an ion pair with protonated amines.

DLS experiments showed that when a solution of p(DAB–Bz) (0.9 mg/ml) was vortexed for 5 s and left standing for 30 min, a high amount of nanoparticles (13,420 kCps) were formed with sizes in the range of 227 nm and small polydispersity index (PDI). This self-aggregation was much less apparent for the boronic acid containing polymers p(DAB–4CPBA) and p(DAB–2AMPBA) where count rates were tenfold and hundredfold lower, respectively. The lower tendency for self-aggregation is most likely due to a more hydrophilic character of these polymers, as the boronic acid groups can form additional hydrogen bonds. Although the presence of the boronic acid moieties apparently reduces the tendency for self-aggregation, the surface charge of the nanoparticles of p(DAB–Bz) and p(DAB–4CPBA) is almost the same with zeta potentials of 40 mV and 43 mV, respectively. This indicates that in both types of nanoparticles the outer sphere is primarily formed by the protonated primary aminobutyl side groups of the polymers.

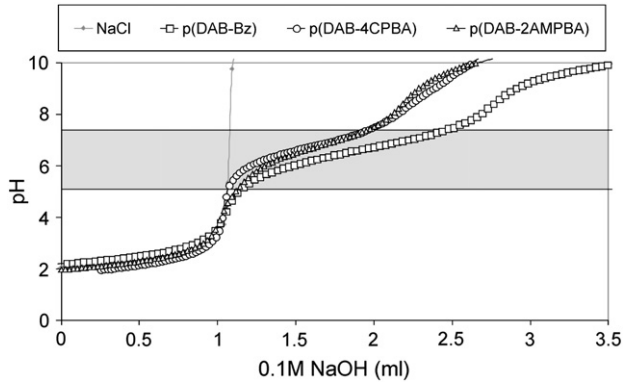

Fig. 1. pH titration curves of 150 mM NaCl (grey diamonds), p(DAB–Bz) (squares), p(DAB–4CPBA) (circles), and p(DAB–2AMPBA) (triangles). Relevant endosomal pH interval between pH 7.4 and 5.1 is marked grey for clarity.

3.3. Polyplex formation

Polyplexes were prepared by adding a polymer solution to a DNA solution at different polymer/DNA weight ratios. Both size and surface potential were determined by dynamic light scattering, and the results are presented in Fig. 2. From Fig. 2A it can be observed that the size of polyplexes of p(DAB–Bz) increased with increasing polymer/DNA weight ratio and thus with increasing polymer concentration. This is not observed for the boronic acid polymers. Already at low polymer/DNA ratio 6/1 both p(DAB–4CPBA) and p(DAB–2AMPBA) form stable and monodisperse nanoparticles smaller than 100 nm that remain of the same size at increasing polymer concentration.

In Figure B polydispersity indices are given in bars and the derived count rates (kCps) of the same polyplexes are given in symbols for polyplexes of p(DAB–Bz) (black and squares), p(DAB–4CPBA) (grey and circles), and p(DAB–2AMPBA) (light grey and triangles). Lines are added for clarity.

Table 1
Polymer properties.

Polymer	M_w (g/mol)	Buffer capacity	Average Size (nm)[a]	Derived count rate (kCps)	PDI[a]	ζ-potential (mV)[a]
p(DAB–Bz)	2730	62%	227 ± 8	13420 ± 60	0.15 ± 0.02	40 ± 2
p(DAB–4CPBA)	2150	44%	72 ± 3	944 ± 5	0.47 ± 0.05	43 ± 3
p(DAB–2AMPBA)	4260	36%	133 ± 65[b]	97 ± 2	0.22 ± 0.04	10 ± 3[b]

[a] Self-assembled nanoparticles formed at polymer concentration 0.9 mg/ml in HEPES (pH 7.4, 20 mM).
[b] Poor data due to low signal.

From Fig. 2B it can be seen that the polydispersity index for polyplexes of p(DAB–Bz) is significantly higher than for the boronic acid containing polymers p(DAB–4CPBA) and p(DAB–2AMPBA). Moreover the number of particles represented by the derived count rate is approximately twice as high for polyplexes of p(DAB–Bz) compared to polyplexes of p(DAB–4CPBA) and p(DAB–2AMPBA), indicating that boronic acid group promotes the formation of well-defined monodisperse particles. As was already discussed in Section 3.2 (Table 1), p(DAB–Bz) has a strong tendency for self-aggregation to form nanoparticles with average size of 227 nm. Therefore, it is likely that also the co-existence of these self-assembled nanoparticles besides the p(DAB–Bz)/DNA polyplexes contribute to the observed higher polydispersity index of p(DAB–Bz). DLS monitoring of a solution containing polyplexes of p(DAB–2AMPBA) at 48/1 polymer/DNA weight ratio showed that stable polyplexes have already formed within the first 5 min after vortexing a fresh solution and both size and count rate (representing the number of particles) remained essentially constant during the next 2 h (Figure S2).

In order to obtain further information on the contribution of the boronic acid moieties to the DNA condensation, polyplexes formed at a 6/1, 12/1, 24/1 and 48/1 polymer/DNA weight ratio were subjected to the ethidium bromide assay (Fig. 3). The ethidium cation gives an increased fluorescence upon intercalation with DNA; therefore the relative decrease in fluorescent signal gives a measure for the fraction of DNA that is not accessible and thus shielded in the polyplex. DNA condensation is a function of the polymer/DNA charge ratio as well as polymer flexibility and molecular weight of the polymer. Since the polymer backbone is the same and the degrees of functionalization of the aminobutyl side chains as well as the M_w of the polymers are similar, differences can be ascribed to the functional groups in the side chains.

At high polymer/DNA weight ratio of 48/1 all three p(DAB) derivatives showed residual ethidium fluorescence of less than 25%, suggesting that >75% of the DNA is effectively shielded from ethidium intercalation inside the polyplex. At lower polymer/DNA weight ratios of 6/1 and 12/1 the boronic acid containing polymers p(DAB–4CPBA) and p(DAB–2AMPBA) were better capable of DNA shielding than p(DAB–Bz), suggesting a more condensed packing of DNA in these boronated polyplexes. From these results it can be concluded that the presence of the boronic acid moieties favorably contributes to effective DNA condensation.

3.4. Atomic force microscopy study of polyplexes formed with p(DAB–2AMPBA)

The polyplexes formed with p(DAB–2AMPBA) at 48/1 polymer/DNA weight ratio were further investigated with atomic force

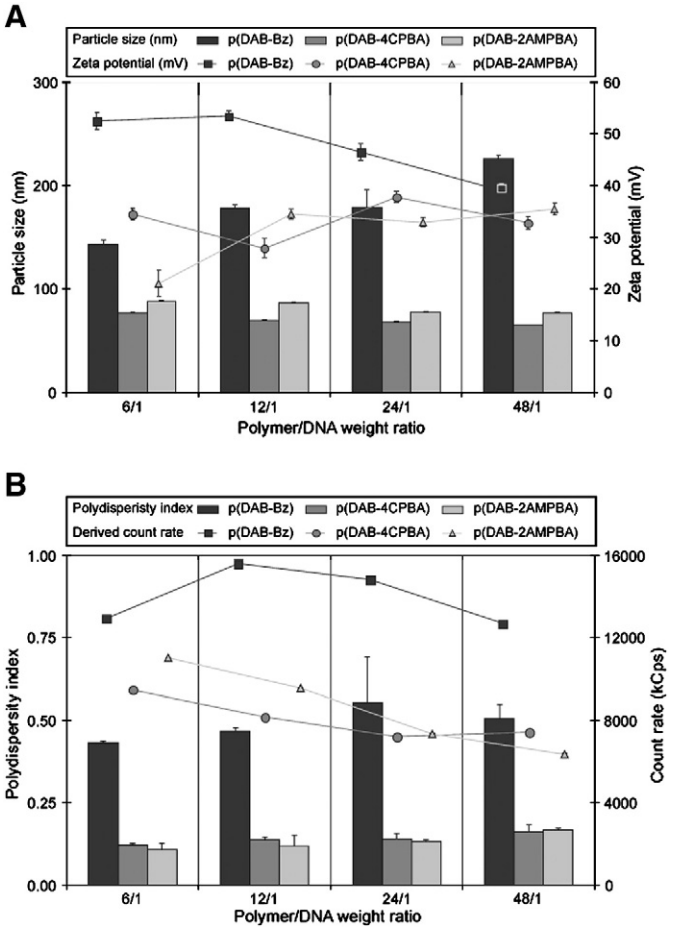

Fig. 2. Polyplexes formed by the different polymers with pDNA. In Figure A polyplex sizes are given in bars and the zeta potentials of the same polyplexes are given in symbols for polyplexes of p(DAB–Bz) (black and squares), p(DAB–4CPBA) (grey and circles), and p(DAB–2AMPBA) (light grey and triangles).

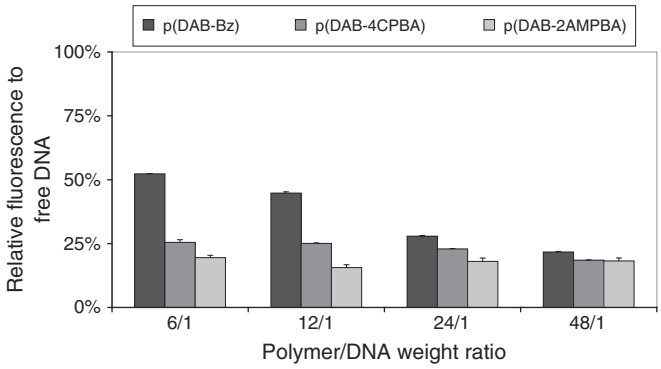

Fig. 3. Fluorescence resulting from ethidium bromide DNA intercalation relative to free pDNA for polyplexes of p(DAB–Bz) (black), p(DAB–4CPBA) (grey), and p(DAB–2AMPBA) (light grey).

microscopy (AFM). A freshly prepared solution polymer/DNA at 48/1 weight ratio in HEPES buffer was added onto a freshly cleaved mica surface and the sample was probed by AFM in tapping mode *in situ* for 3 h. Next, the sample was dried overnight and measured again the day after in the dry state.

At the start of the measurement, predominantly plasmid DNA was visible at the surface and after 2 to 3 h an increasing number of polyplex aggregates could be observed (Fig. 4). This slow polyplex formation at the surface is significantly different from that observed for the polyplexes formed in solution, as studied by DLS. This may be due to the adsorption of the positively charged polymer on the negatively charged mica surface. In Fig. 4A,B predominantly uncondensed plasmid DNA is visible. By following the same DNA plasmids for 2 h it was observed that the DNA gradually condensed into spherical particles with heights up to 40 – 80 nm. At first, loosely packed particles with uncondensed DNA coils at the periphery of the polyplexes and much denser packed material (DNA and polymer) on the inside were apparent and progressing in time the polyplexes became more homogeneously densely packed. In Fig. 4C a semi condensed or "immature" polyplex with a height of 10 nm is depicted, which slowly became more condensed with a height of 48 nm after another 30 min (inset in Fig. 4C). In the phase image (Fig. 4D) the softer "free" DNA appears light and the more rigid core appears as darker spots (inset in Fig. 4D). When the sample was rinsed with HEPES buffer and left drying overnight spherical particles could be observed in Fig. 4E and F, where no phase contrast was observed, indicating that the particles were homogeneously packed.

Cross section analysis of 15 polymer/DNA particles on the mica surface gave an average diameter of 138 ± 64 nm. For comparison, also polymer in absence of DNA was measured. It was found that the polymer slowly adsorbed to the mica surface forming aggregates with a much smaller averaged diameter of 28 ± 6 nm (cross section analysis of 10 particles) (data not shown).

3.5. Transfection studies

Transfection efficiencies of polyplexes of the polymers with DNA encoding for green fluorescent protein (GFP) were determined by measuring the fluorescent intensities in COS-7 cells both in the absence and in the presence of serum. The cell viabilities of the corresponding polyplexes were determined by XTT-assay. Fig. 5A shows the transfection and cell viabilities in the absence of serum. From this figure it is clear that polyplexes of p(DAB–Bz) showed the highest transfections with 2–3 times higher than those obtained with polyplexes from the reference polymer linear PEI (Exgen) at its optimal N/P ratio 6. Polyplexes of p(DAB–4CPBA) showed similar transfection efficiencies as Exgen, whereas polyplexes of p(DAB–2AMPBA) were not very efficient in the transfection. The lower transfection efficiency of the boronic acid functionalized polymers compared to the non-boronated analog p(DAB–Bz) may be primarily caused by the higher cytotoxicity that is observed for these polyplexes. Whereas p(DAB–Bz) shows almost no cytotoxicity at 6/1, 12/1 and 24/1 polymer/DNA weight ratios, the cell viabilities of

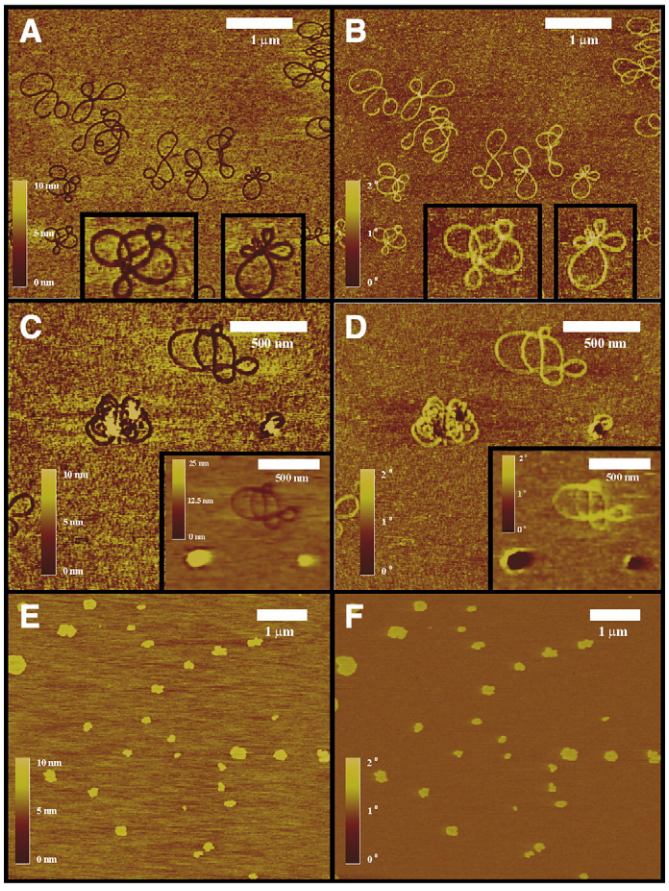

Fig. 4. Atomic force microscopy height images (A,C,E) and phase images (B,D, F) of polyplexes with p(DAB–2AMPBA) in tapping mode. (A,B) Onset of particle formation of DNA polyplexes on mica in HEPES buffer. (C,D) Second stage (after 1.5 h) of DNA polyplex wrapping process. Note the condensed particles in the insets that have been formed after 2 h. The outsides of the particles show clear phase contrast indicating less dense and more adhesive material. (E, F) Final stage of the condensed particles after 1 day measured in dry air.

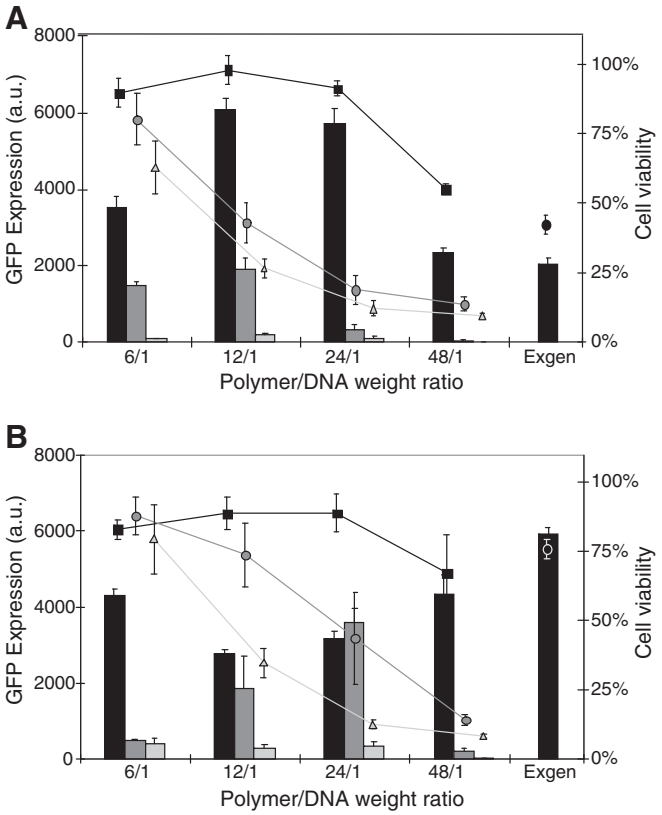

Fig. 5. Transfection efficiencies in COS-7 cells (fluorescence from GFP expression is shown in bars) and cell viabilities of the same polyplexes (metabolic activity by XTT relative to untreated cells is shown in symbols) in the absence of serum (A) and in the presence of serum (B). Polyplexes were prepared with p(DAB–Bz) (black and squares), p(DAB–4CPBA) (grey and circles), and p(DAB–2AMPBA) (light grey and triangles). Lines are added for clarity.

p(DAB–4CPBA) and p(DAB–2AMPBA) strongly decrease with increasing polymer/DNA weight ratio.

The transfection and cell viabilities in the presence of serum give a different outcome (Fig. 5B). A higher GFP expression for Exgen in the presence of serum than in the absence of serum was to be expected as this formulation is optimized for use in the presence of serum according to the manufacturer. Remarkably, polyplexes of p(DAB–Bz) at all polymer/DNA ratios and polyplexes of p(DAB–4CPBA) at 12/1 and 24/1 ratio show good transfection efficiencies in the presence of serum. Generally, the presence of serum impedes the transfection efficiency of cationic polyplexes. Therefore, these polymers can be considered as potent gene delivery vectors in the presence of serum, with efficiencies comparable to that of Exgen. The increase in GFP expression for p(DAB–4CPBA) can be explained by the improved cell viability in the presence of serum. In serum the 4CPBA groups are probably (partially) shielded, giving rise to lower cytotoxicity. In contrast, the cytotoxicity profile of polyplexes of p(DAB–2AMPBA) is only slightly improved in presence of serum and the only marginal increases in transfection efficiency are observed in this medium. The 2AMPBA moiety binds stronger to diols than the 4CPBA moiety at physiological pH, and therefore stronger interference with cellular integrety might be caused by the p(DAB–2AMPBA) polyplexes.

3.6. Hemolytic activity of the polymers

The presence of boronic acid moieties in the p(DAB–4CPBA) and p(DAB–2AMPBA) polymers showed to induce an increased cytotoxicity, especially for polyplexes of p(DAB–2AMPBA). Since boronic acids bind to vicinal diols, as are present in carbohydrates, it is likely that the boronated polyplexes interact with glycoproteins on the cell surface [37–39]. Boronic ester formation with the glycocalix of the cells could improve membrane adhesion and consequently could promote particle uptake, as is schematically illustrated in Fig. 6. However, the increased interaction of the boronic acid moieties with extracellular or intracellular membranes could also give rise to interference with essential membrane processes or even membrane disruption and thereby induce toxicity.

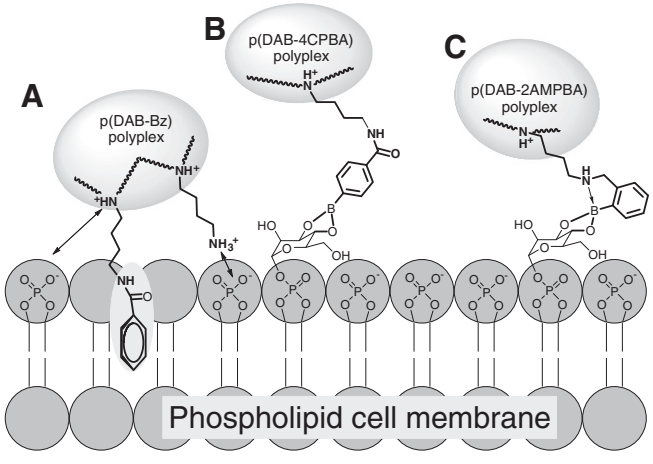

Fig. 6. Schematic representation of possible interactions between polyplexes and cells. A: Hydrophobic interaction of the benzoylated side chains with the hydrophobic phospholipids of the cell membrane in combination with charge attraction of the protonated aminobutyl side chains with the negatively charged phospolipid membrane. B: Boronic ester formation of 4-carbamoylphenylboronic acid side chains with a carbohydrate residue on the cell surface. C: Enhanced boronic ester formation through dative B–N interaction of *2*-aminomethylphenylboronic acid side chains with a carbohydrate residue of the cell surface.

In order to obtain more information about the membrane disrupting activity of the polymers, a hemolytic red blood cell (RBC) assay was performed. In this assay the concentration of hemoglobin is determined that leaked out of the erythrocytes due to the polymer-induced disruption of the erythrocyte cell membrane. The hemolytic activity of the polymers serves as an indication for the membrane disruptive properties of the polymer. To investigate the role of the presence of boronic acid moieties in this process, polymer dilution series were prepared of the non-boronated p(DAB–Bz) as well as of the boronated polymers p(DAB–4CPBA) and p(DAB–2AMPBA). The polymer solutions were added to erythrocytes and the hemoglobin concentration of the supernatant was measured using UV-absorption and compared with complete lysis with Triton X–100. The data points in Fig. 7 for the non-boronated polymer p(DAB–Bz) show that significant hemolytic activity becomes apparent at polymer concentration above 0.05 mg/ml. This hemolytic activity may originate from cationic interactions of the protonated aminobutyl side chains and from hydrophobic interactions of the benzoyl groups with the cell membrane.

Remarkably, the boronated polymer p(DAB–4CPBA) has significantly less hemolytic activity which was unexpected based on the cell viabilities of the polyplexes. A possible reason for the lower hemolytic activity could be the reduced hydrophobicity of the 4-carbamoylphenylboronic acid group (4CPBA) as compared to the benzoyl group. Polymer p(DAB–2AMPBA) with the ortho-aminophenylboronic acid (2AMPBA) exhibits significantly higher hemolytic activity, which is already starting at a much lower polymer concentration. This observation may serve as an indication that the 2AMPBA groups induce stronger membrane interactions than the 4CPBA groups, which is in accordance with higher propensity of the 2AMPBA groups for boronic ester formation. These stronger membrane interactions could then be well responsible for the high cytotoxicity of the polyplexes formed with p(DAB–2AMPBA) as was observed by the XTT assays.

4. Conclusions

The grafting of 30% of the aminogroups in the side chains of p(DAB) with boronic acid moieties, yielding p(DAB–4CPBA) and p(DAB–2AMPBA), resulted in the formation of smaller and more monodisperse polyplexes compared to the non-boronated p(DAB–Bz). Moreover, shielding against ethidium intercalation indicates a more efficient condensation and packing of DNA by the boronated polymers. In the absence of serum, polyplexes of the benzoylated

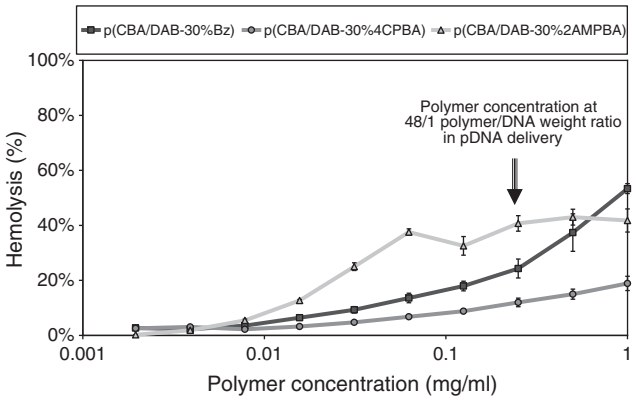

Fig. 7. Hemolytic activity of the polymer p(DAB–Bz) (squares), p(DAB–4CPBA) (circles) and p(DAB–2AMPBA) (triangles) as determined by the RBC assay. Positive control triton X-100 (1 mg/ml) was set to 100% and negative control HBS was set to 0%. Lines are added for clarity and the arrow represents the highest polymer concentration used in the transfection assay (at 48/1 polymer/DNA weight ratio).

polymer p(DAB–Bz) showed 2–3 times higher transfections than PEI, whereas p(DAB–4CPBA) gave about equal transfection efficiencies. Although the presence of serum frequently reduces transfection efficiency, for p(DAB–4CPBA) the transfection efficiency was considerably improved compared to the serum-free medium, which may due to the lower cytotoxicity observed. The remarkable low transfection efficiency and cell viability of p(DAB–2AMPBA) polyplexes can be related to the significantly higher hemolytic activity of this polymer, and serve as an indication that the 2AMPBA moieties induce stronger membrane interactions leading to membrane disruption or interference with essential cellular processes.

In conclusion, the presence of phenylboronic acid moieties in the side chains of the poly(amidoamine)s promote the formation of small and monodisperse polyplexes that are stable in time. Plasmid DNA is effectively shielded in these polyplexes. However, the amount of boronated groups and the polymer/DNA ratio of the polyplexes have to be carefully optimized since the boronated polymers appear to be less tolerable to cytotoxicity than their non-boronated analog. An interesting feature of the presence of boronic acid moieties in these polymers is that reversible boronate ester formation opens the possibility for improved mucoadhesion, (glyco)targeting, and decoration of the polyplexes with a variety of polyols such as oligo- and polysaccharides providing stealth properties. The exploration of these possibilities is subject of further studies.

Acknowledgement

The authors thank Hans van der Aa for his help with the hemolytic assay, Tieme Stevens for the M_w determination of the polymers, and Anika Embrechts for the atomic force microscopy measurements.

Appendix A. Supplementary data

Supplementary data to this article can be found online at doi:10.1016/j.jconrel.2011.07.011.

References

[1] I.M. Verma, N. Somia, Gene therapy – promises, problems and prospects, Nature 389 (1997) 239–242.
[2] O. Singer, I.M. Verma, Applications of lentiviral vectors for shRNA delivery and transgenesis, Curr. Gene Ther. 8 (2008) 483–488.
[3] S.Y. Wong, J.M. Pelet, D. Putnam, Polymer systems for gene delivery-past, present, and future, Prog. Polym. Sci. 32 (2007) 799–837.
[4] E. Wagner, J. Kloeckner, Gene delivery using polymer therapeutics, Adv. Polym. Sci. 192 (2006) 135–173.
[5] S.B. Zhang, Y.M. Xu, B. Wang, W.H. Qiao, D.L. Liu, Z.S. Li, Cationic compounds used in lipoplexes and polyplexes for gene delivery, J. Control. Release 100 (2004) 165–180.
[6] J. Luten, C.F. van Nostruin, S.C. De Smedt, W.E. Hennink, Biodegradable polymers as non-viral carriers for plasmid DNA delivery, J. Control. Release 126 (2008) 97–110.
[7] T.G. Park, J.H. Jeong, S.W. Kim, Current status of polymeric gene delivery systems, Adv. Drug Deliver. Rev. 58 (2006) 467–486.
[8] P. Ferruti, M.A. Marchisio, R. Duncan, Poly(amido-amine)s: biomedical applications, Macromol. Rapid Comm. 23 (2002) 332–355.
[9] C. Lin, Z.Y. Zhong, M.C. Lok, X.L. Jiang, W.E. Hennink, J. Feijen, J.F.J. Engbersen, Linear poly(amido amine)s with secondary and tertiary amino groups and variable amounts of disulfide linkages: synthesis and in vitro gene transfer properties, J. Control. Release 116 (2006) 130–137.
[10] C. Lin, Z.Y. Zhong, M.C. Lok, X.L. Jiang, W.E. Hennink, J. Feijen, J.F.J. Engbersen, Novel bioreducible poly(amido amine)s for highly efficient gene delivery, Bioconjugate Chem. 18 (2007) 138–145.
[11] M. Piest, C. Lin, M.A. Mateos-Timoneda, M.C. Lok, W.E. Hennink, J. Feijen, J.F.J. Engbersen, Novel poly(amido amine)s with bioreducible disulfide linkages in their diamino-units: structure effects and in vitro gene transfer properties, J. Control. Release 130 (2008) 38–45.
[12] C. Lin, C.J. Blaauboer, M.M. Timoneda, M.C. Lok, M. van Steenbergen, W.E. Hennink, Z.Y. Zhong, J. Feijen, J.F.J. Engbersen, Bioreducible poly(amido amine)s with oligoamine side chains: synthesis, characterization, and structural effects on gene delivery, J. Control. Release 126 (2008) 166–174.
[13] M.A. Mateos-Timoneda, M.C. Lok, W.E. Hennink, J. Feijen, J.F.J. Engbersen, Poly (amido amine)s as gene delivery vectors: Effects of quaternary nicotinamide moieties in the side chains, Chem. Med. Chem. 3 (2008) 478–486.
[14] M. Piest, J.F.J. Engbersen, Effects of charge density and hydrophobicity of poly (amido amine)s for non-viral gene delivery, J. Control. Release 148 (2010) 83–90.
[15] W.Q. Yang, X.M. Gao, B.H. Wang, Boronic acid compounds as potential pharmaceutical agents, Med. Res. Rev. 23 (2003) 346–368.
[16] S.L. Wiskur, J.J. Lavigne, H. Ait-Haddou, V. Lynch, Y.H. Chiu, J.W. Canary, E.V. Anslyn, pK(a) values and geometries of secondary and tertiary amines complexed to boronic acids – implications for sensor design, Org. Lett. 3 (2001) 1311–1314.
[17] H. Kitano, M. Kuwayama, N. Kanayama, K. Ohno, Interfacial recognition of sugars by novel boronic acid-carrying amphiphiles prepared with a lipophilic radical initiator, Langmuir 14 (1998) 165–170.
[18] A. Matsumoto, S. Ikeda, A. Harada, K. Kataoka, Glucose-responsive polymer bearing a novel phenylborate derivative as a glucose-sensing moiety operating at physiological pH conditions, Biomacromolecules 4 (2003) 1410–1416.
[19] T. Hoare, R. Pelton, Engineering glucose swelling responses in poly(N-isopropylacrylamide)-based microgels, Macromolecules 40 (2007) 670–678.
[20] B. Appleton, T.D. Gibson, Detection of total sugar concentration using photoinduced electron transfer materials: development of operationally stable, reusable optical sensors, Sensor Actuat. B-Chem. 65 (2000) 302–304.
[21] S.H. Gao, W. Wang, B.H. Wang, Building fluorescent sensors for carbohydrates using template-directed polymerizations, Bioorg. Chem. 29 (2001) 308–320.
[22] M. Di Luccio, B.D. Smith, T. Kida, C.P. Borges, T.L.M. Alves, Separation of fructose from a mixture of sugars using supported liquid membranes, J. Membrane Sci. 174 (2000) 217–224.
[23] A.E. Ivanov, I.Y. Galaev, B. Mattiasson, Binding of adenosine to pendant phenylboronate groups of thermoresponsive copolymer: a quantitative study, Macromol. Biosci. 5 (2005) 795–800.
[24] A. Ozdemir, A. Tuncel, Boronic acid-functionalized HEMA-based gels for nucleotide adsorption, J. Appl. Polym. Sci. 78 (2000) 268–277.
[25] H. Cicek, Nucleotide isolation by boronic acid functionalized hydrogel beads, J. Bioact. Compat. Pol. 20 (2005) 245–257.
[26] S. Senel, S.T. Camli, M. Tuncel, A. Tuncel, Nucleotide adsorption-desorption behaviour of boronic acid functionalized uniform-porous particles, J. Chromatogr. B 769 (2002) 283–295.
[27] B. Elmas, M.A. Onur, S. Senel, A. Tuncel, Temperature controlled RNA isolation by N-isopropylacrylamide-vinylphenyl boronic acid copolymer latex, Colloid Polym. Sci. 280 (2002) 1137–1146.
[28] A. Coskun, E.U. Akkaya, Three-point recognition and selective fluorescence sensing of L-DOPA, Org. Lett. 6 (2004) 3107–3109.
[29] S. Kitano, Y. Koyama, K. Kataoka, T. Okano, Y. Sakurai, A novel drug delivery system utilizing a glucose responsive polymer complex between poly(vinyl alcohol) and poly(N-vinyl-2-pyrrolidone) with a phenylboronic acid moiety, J. Control. Release 19 (1992) 161–170.
[30] C. Young Kweon, J. Seo Young, K. Young Ha, A glucose-triggered solubilizable polymer gel matrix for an insulin delivery system, Int. J. Pharm. 80 (1992) 9–16.
[31] D. Shiino, Y. Murata, K. Kataoka, Y. Koyama, M. Yokoyama, T. Okano, Y. Sakurai, Preparation and characterization of a glucose-responsive insulin-releasing polymer device, Biomaterials 15 (1994) 121–128.
[32] D. Shiino, Y. Murata, A. Kubo, Y.J. Kim, K. Kataoka, Y. Koyama, A. Kikuchi, M. Yokoyama, Y. Sakurai, T. Okano, Amine containing phenylboronic acid gel for glucose-responsive insulin release under physiological pH, J. Control. Release 37 (1995) 269–276.
[33] V. Lapeyre, C. Ancla, B. Catargi, V. Ravaine, Glucose-responsive microgels with a core-shell structure, J. Colloid Interface Sci. 327 (2008) 316–323.
[34] T. Koyama, K. Terauchi, Synthesis and application of boronic acid-immobilized porous polymer particles: a novel packing for high-performance liquid affinity chromatography, J. Chromatogr. B 679 (1996) 31–40.
[35] S.J. Coutts, T.A. Kelly, R.J. Snow, C.A. Kennedy, R.W. Barton, J. Adams, D.A. Krolikowski, D.M. Freeman, S.J. Campbell, J.F. Ksiazek, W.W. Bachovchin, Structure-activity relationships of boronic acid inhibitors of dipeptidyl peptidase IV.1. Variation of the P-2 position of X(aa)-boroPro dipeptides, J. Med. Chem. 39 (1996) 2087–2094.
[36] P. Hazot, T. Delair, A. Elaissari, J.P. Chapel, C. Pichot, Functionalization of poly(N-ethylmethacryl-amide) thermosensitive particles by phenylboronic acid, Colloid Polym. Sci. 280 (2002) 637–646.
[37] N.D. Winblade, H. Schmokel, M. Baumann, A.S. Hoffman, J.A. Hubbell, Sterically blocking adhesion of cells to biological surfaces with a surface-active copolymer containing poly(ethylene glycol) and phenylboronic acid, J. Biomed. Mater. Res. 59 (2002) 618–631.
[38] Y.R. Vandenburg, Z.Y. Zhang, D.J. Fishkind, B.D. Smith, Enhanced cell binding using liposomes containing an artificial carbohydrate-binding receptor, Chem. Commun. (2000) 149–150.
[39] A.E. Ivanov, I.Y. Galaev, B. Mattiasson, Interaction of sugars, polysaccharides and cells with boronate-containing copolymers: from solution to polymer brushes, J. Mol. Recognit. 19 (2006) 322–331.
[40] A.E. Ivanov, K. Shiomori, Y. Kawano, I.Y. Galaev, B. Mattiasson, Effects of polyols, saccharides, and glycoproteins on thermoprecipitation of phenylboronate-containing copolymers, Biomacromolecules 7 (2006) 1017–1024.
[41] H. Otsuka, E. Uchimura, H. Koshino, T. Okano, K. Kataoka, Anomalous binding profile of phenylboronic acid with N-acetylneuraminic acid (Neu5Ac) in aqueous solution with varying pH, J. Am. Chem. Soc. 125 (2003) 3493–3502.
[42] M.R. Dreher, W. Liu, C.R. Michelich, M.W. Dewhirst, F. Yuan, A. Chilkoti, Tumor vascular permeability, accumulation, and penetration of macromolecular drug carriers, J. Natl. Cancer Inst. 98 (2006) 335–344.
[43] A. Matsumoto, H. Cabral, N. Sato, K. Kataoka, Y. Miyahara, Assessment of tumor metastasis by the direct determination of cell-membrane sialic acid expression, Angew. Chem. Int. Ed. 49 (2010) 5494–5497.

[44] S. Moffatt, S. Wiehle, R.J. Cristiano, Tumor-specific gene delivery mediated by a novel peptide-polyethylenimine-DNA polyplex targeting aminopeptidase N/CD13, Hum. Gene Ther. 16 (2005) 57–67.
[45] S. Moffatt, R.J. Cristiano, Uptake characteristics of NGR-coupled stealth PEI/pDNA nanoparticles loaded with PLGA-PEG-PLGA tri-block copolymer for targeted delivery to human monocyte-derived dendritic cells, Int. J. Pharmaceut. 321 (2006) 143–154.
[46] Q. Peng, F. Chen, Z. Zhong, R. Zhuo, Enhanced gene transfection capability of polyethylenimine by incorporating boronic acid groups, Chem. Commun. 46 (2010) 5888–5890.